INTERNATIONAL JOURNAL OF GEOMAGNETISM AND AERONOMY
VOL. 2, NO. 3, PAGES 159–172, DECEMBER 2001

Determination of FAC patterns in the daytime cusp region with regard to edge effects of current sheets

R. Lukianova and O. Troshichev

Arctic and Antarctic Research Institute, St. Petersburg, Russia

Yu. Galperin and N. Jorjio

Institute of Space Research, Moscow, Russia

Abstract. A numerical method of reconstruction of field-aligned currents (FAC), taking into account both, zonal and meridional, components of the magnetic perturbations observed along the spacecraft trajectory, has been developed. While a zonal component specifies the number, polarity, and latitudinal location of FAC sheets, a meridional component is evidence of edges and gaps in the current sheets. The model simulation was used to derive general regularities in variations of zonal and meridional components in case of one, two, three and four longitudinally limited current sheets, the two-dimensional equation for vector magnetic potential being solved numerically in spherical coordinates. Transverse magnetic field disturbances observed by the AUREOL 3 and magnetic field components calculated at the footpoints of projection of satellite trajectory are compared. Parameters of a FAC pattern (number of sheets, polarity, intensity, location) are modified in the way that curves match best. A set of optimal parameters is derived from the solution of equations for local minimums. FAC patterns obtained from the AUREOL 3 data for interplanetary magnetic field conditions $B_z > 0$ and $B_y = 0$ show the following features: There are two additional current sheets located poleward of traditional Region 1 FAC. These sheets consist of pairs of the oppositely directed currents separated by a gap at the noon meridian. The conclusion is made that a four-layer current structure (FAC Regions 2 and 1 and two sheets poleward of Region 1) can be observed under conditions $B_z > 0$ and $B_y = 0$ in prenoon and afternoon magnetic local time sectors simultaneously.

1. Introduction

The basic scheme of field-aligned currents (FAC) distribution in the dayside polar region was presented by *Iijima and Potemra* [1976]. This scheme shows availability of the following three current sheets: Region 2 FAC at the low-latitude edge of the auroral oval, Region 1 FAC at the high-latitude edge of the oval, and the cusp FAC region located poleward of Region 1. The original scheme of *Iijima and Potemra* [1976] did not specify the influence of the interplanetary magnetic field (IMF) B_y component and Region 1 FAC and currents poleward of Region 1 were regarded as two independent systems. *McDiarmid et al.* [1979] put forward a specific model in which the poleward sheet of field-aligned currents was considered as an extension of Region 1 across the noon meridian under the influence of IMF azimuthal component. The difference between these two basic patterns is of fundamental importance: in the first case [*Iijima and Potemra*, 1976], the cusp FACs and Region 1 FAC have different sources, while in the second case [*McDiarmid et al.*,

Paper number GAI00353.
CCC: 1524–4423/2001/0203–0353$18.00

The online version of this paper was published October 5, 2001.
URL: http://ijga.agu.org/v02/gai00353/gai00353.htm
Print companion issued December 2001.

1979], their source is the same. All subsequent FAC patterns in the dayside cusp region succeed these two patterns [*D'Angelo*, 1980; *de la Beaujardiere et al.*, 1993; *Doyle et al.*, 1981; *Erlandson et al.*, 1988; *Friis-Christensen et al.*, 1985; *Levitin et al.*, 1982; *Ohtani et al.*, 1995a, 1995b; *Saflekos et al.*, 1982; *Saunders*, 1992; *Taguchi et al.*, 1993; *Troshichev et al.*, 1982, 1996; *Watanabe et al.*, 1996; *Yamauchi et al.*, 1993]. In spite of the escalating number of spacecraft measurements of the field-aligned current effects in the cusp region the determination of the FAC structure continues to be ambiguous up to now because of two main reasons: (1) FAC patterns are reconstructed on the basis of isolated spacecraft traverses through the cusp/cleft region and (2) only the zonal (east-west) component of the magnetic field perturbation is generally taken into account on the implicit assumption that a satellite orbit is perpendicular to extended sheets of currents.

Meanwhile, the results of the simulation analysis of *Lukianova* [1997] have shown that different patterns of the field-aligned currents in the cusp/cleft region, proposed by *Erlandson et al.* [1988], *Saunders* [1992], *Yamauchi et al.* [1993], *Taguchi et al.* [1993], and *Troshichev et al.* [1996], produce a very similar distribution of the meridional (north-south) component of electric field E_θ, which is responsible for the zonal part of convection flows. The zonal (east-west) component of the electric field E_φ responsible for the meridional part of the convection flows turned out to be more sensitive to the choice of the FAC pattern. It means that the meridional component of the transverse magnetic perturbations should be taken into account in analyses of FAC patterns in addition to the zonal component. In this article we present the results of the simulation analysis (profiles of zonal B_E and meridional B_N components of the transverse magnetic perturbations), obtained for specific structures of sources, the effects of near-edge traverse of current sheets being taken into account.

General regularities of B_E and B_N profiles, typical for different current structures, give us a background for the reconstruction of FAC, observed in passes of AUREOL spacecraft in the daytime cusp region. The reconstruction is realized by the method of model calculation and successive approximation of calculated magnetic disturbances to those observed. The multisheet assumption with consideration for edge effects makes the best guess of FAC patterns from only one path of a satellite.

2. Magnetic Perturbations Produced by Model FAC Structures

To derive a set of typical B_E and B_N signatures, we examine the magnetic field perturbations produced by model FAC structures.

2.1. Method of Calculation

The magnetic field can be expressed in terms of a vector-potential as $B = \mathrm{curl}\, A$ with an additional condition $\mathrm{div}\, \mathbf{A} = 0$. If a current is assumed to flow normally to a thin shell of radius r (geocentric altitude of satellite in our case), the vector-potential has only component A_r in coordinates θ (latitude), φ (longitude), and r. The polar cap region is regarded as plane. From the expression $B = \mathrm{curl} A(\theta, \varphi)\mathbf{e}_r$, where $\mathbf{e}_r$ is the unit vector outwardly directed from the center of the Earth, the zonal and meridional components of magnetic field are defined as

$$B_\varphi = -\frac{1}{r}\frac{\partial A}{\partial \theta} \qquad B_\theta = -\frac{1}{r\sin\theta}\frac{\partial A}{\partial \varphi} \tag{1}$$

Using a network of points with $\Delta\varphi$ in longitude and $\Delta\theta$ in latitude for the unit contour around every point of grid (i, j), the components B_φ and B_θ are calculated, respectively,

$$\begin{aligned}
(B_\varphi)_1 &= -\frac{A_{ij} - A_{i-1\,j}}{r\Delta\theta} \\
(B_\varphi)_2 &= -\frac{A_{i+1\,j} - A_{ij}}{r\Delta\theta} \\
(B_\theta)_3 &= \frac{1}{r\sin\theta_i}\frac{A_{ij} - A_{i\,j-1}}{\Delta\varphi} \\
(B_\theta)_4 &= \frac{1}{r\sin\theta_i}\frac{A_{i\,j+1} - A_{ij}}{\Delta\varphi}
\end{aligned} \tag{2}$$

If the current flows through the contour with perimeter L, it will be related to the magnetic field as

$$\oint_L \frac{1}{\mu} B_l dl - \frac{4\pi}{c}\int_s j ds = 0 \tag{3}$$

where j is current density, l is line element, and s is area of the unit contour. By combining (2) and (3), the equation for every grid point is derived. Equations are solved numerically by a finite difference scheme over a network of points spaced $\Delta\theta = 0.5^\circ$ in latitude and $\Delta\varphi = 1^\circ$ in longitude. The main expression for the iteration technique is

$$\begin{aligned}
A_{ij}^{(n+1)} &= A_{ij}^{(n)} - \Delta A_{ij}^{(n,n+1)} \\
\Delta A_{ij}^{(n,n+1)} &= w\frac{f_{ij}(A_{11}^{(n+1)}, \ldots, A_{i-1\,j}^{(n+1)}, A_{ij}^{(n)}, \ldots)}{\frac{\partial}{\partial A_{ij}^{(n)}} f_{ij}(A_{11}^{(n+1)}, \ldots, A_{i-1\,j}, A_{ij}^{(n)})}
\end{aligned} \tag{4}$$

where f is the left-hand side of (3), w is overrelaxation parameter, and n is number of iterations. The boundary condition at the equator boundary $\theta = 30^\circ$ is $A = 0$. To avoid the unnatural condition at the pole, the grid is shifted a half step away from the pole so as not to contain it. Once the distribution of vector potential is obtained, we can derive the magnetic field from (1).

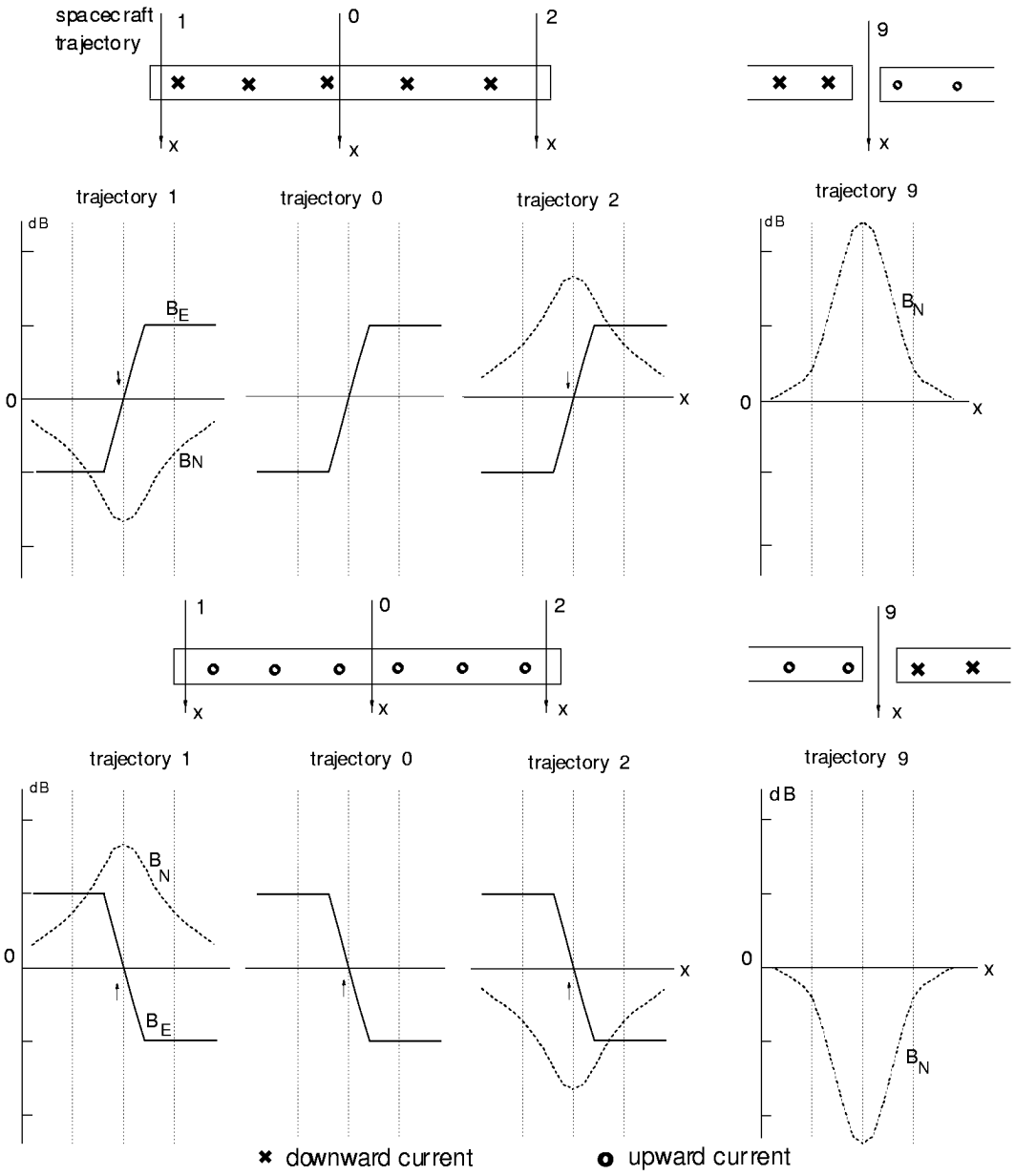

Figure 1. Model pattern of current sheets and profiles of zonal (solid lines) and meridional (dotted lines) components of magnetic perturbation (solid arrows) along trajectories (in the case of one sheet).

2.2. Signatures of Current Sheets in Magnetic B_E and B_N Components

Effects of finite extension of one, two, three, and four current sheets are examined for cases when a spacecraft crosses these sheets at a right angle. Multisheet patterns are schematically represented in Figures 1–4. The following simplifying assumptions are taken in the calculation: All FACs sheets are parallel to each other. Currents in the sheets are of uniform density. The edges of current sheets are of rectangular form. Figures 1–4 show a behavior of the meridional north-south B_N (solid lines) and zonal east-west B_E (dotted lines) components of magnetic perturbation along the ascending spacecraft orbit in case of one (Figure 1), two (Figure 2), three (Figure 3), and four (Figure 4) current sheets. The computation was carried out in the spherical coordinates, but current sheets are presented, for simplicity as rectangular in Figures 1–4. It is common knowledge that just the east-west magnetic component determines the latitudinal position of sheets, their polarity and intensity. If the spacecraft moves toward the pole the positive (negative) trend of B_E indicates downward (upward) currents, the latitudinal width of the trend being indicated as the width of

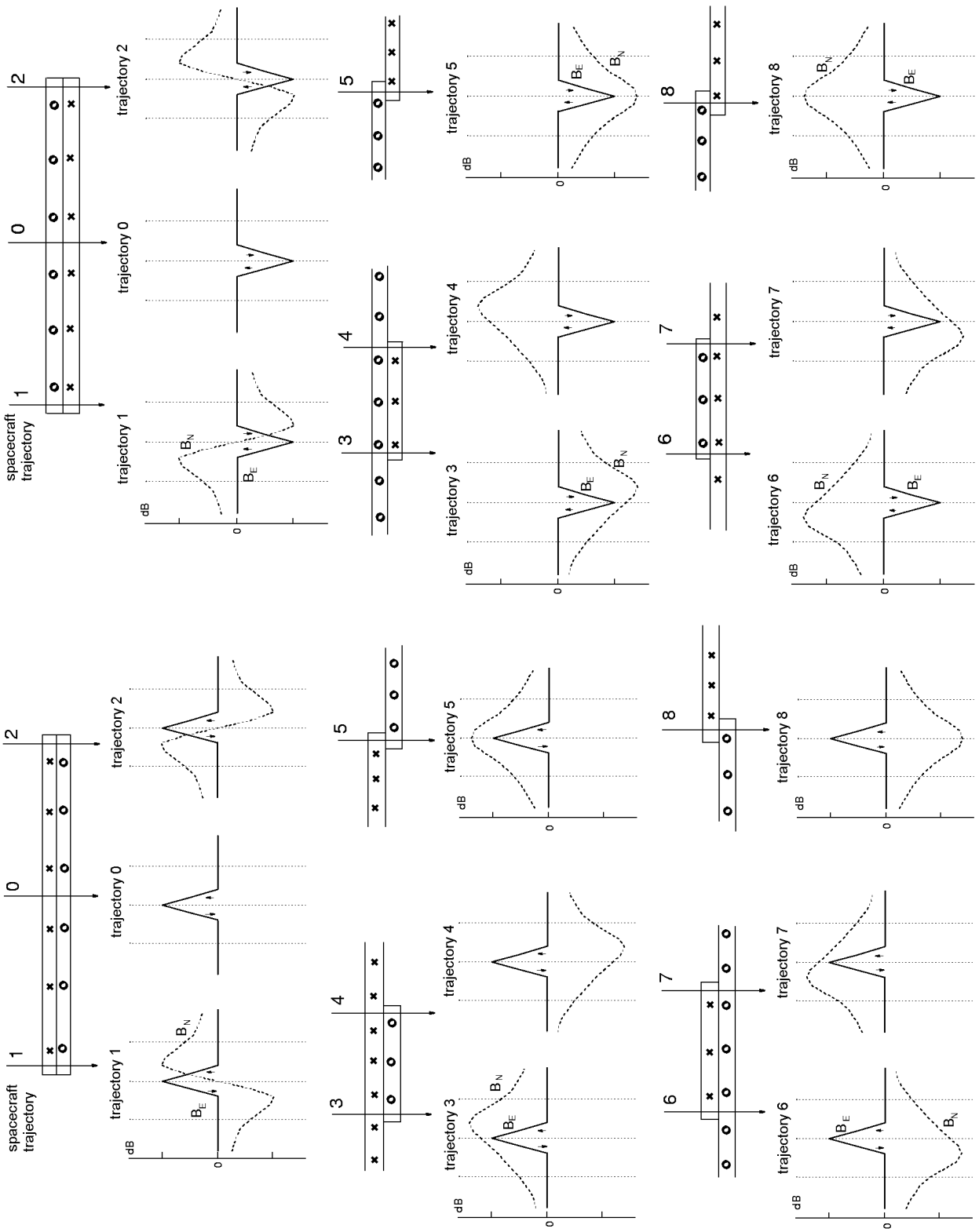

Figure 2. Same as Figure 1 (in the case of two sheets).

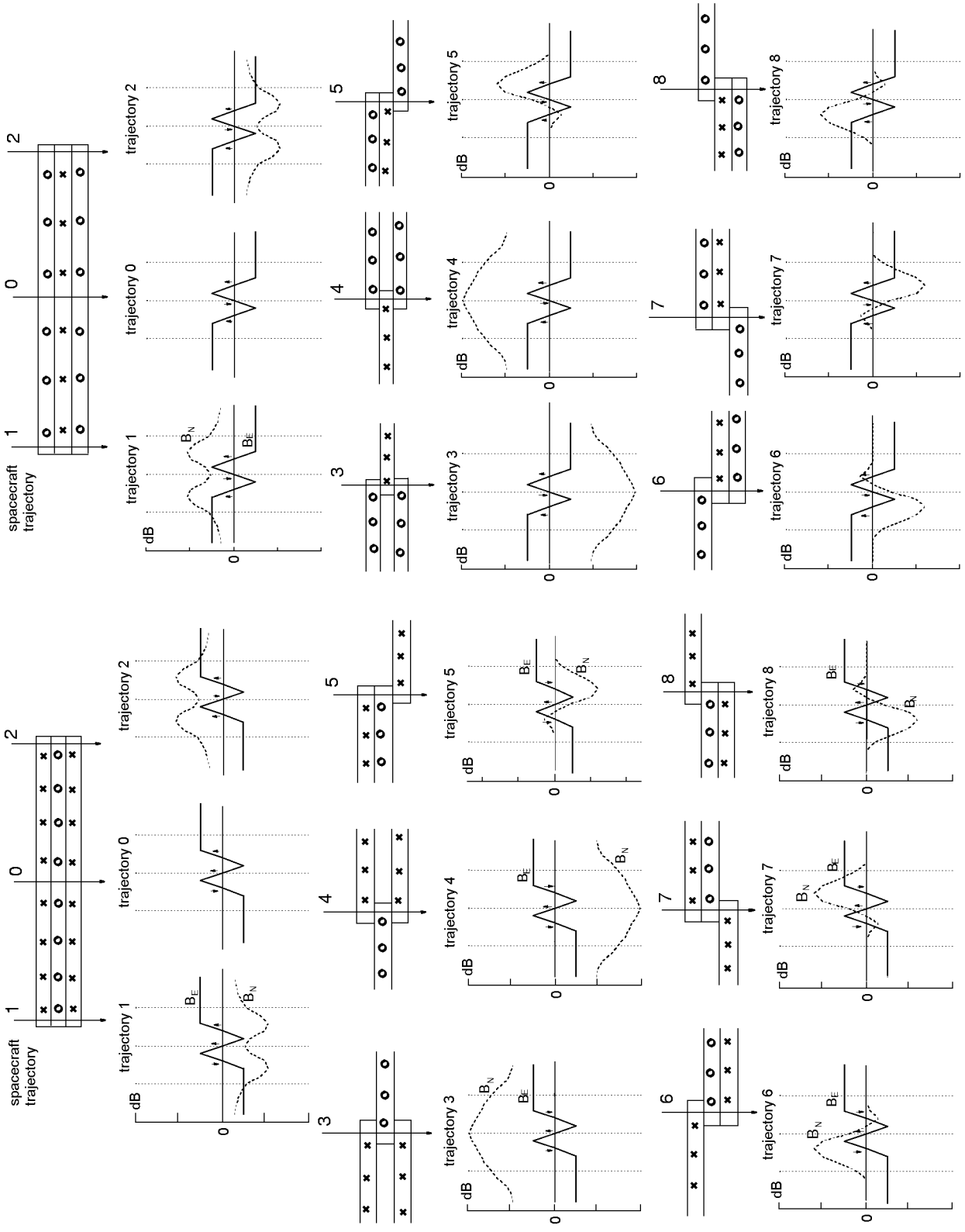

Figure 3. Same as Figure 1 (in the case of three sheets).

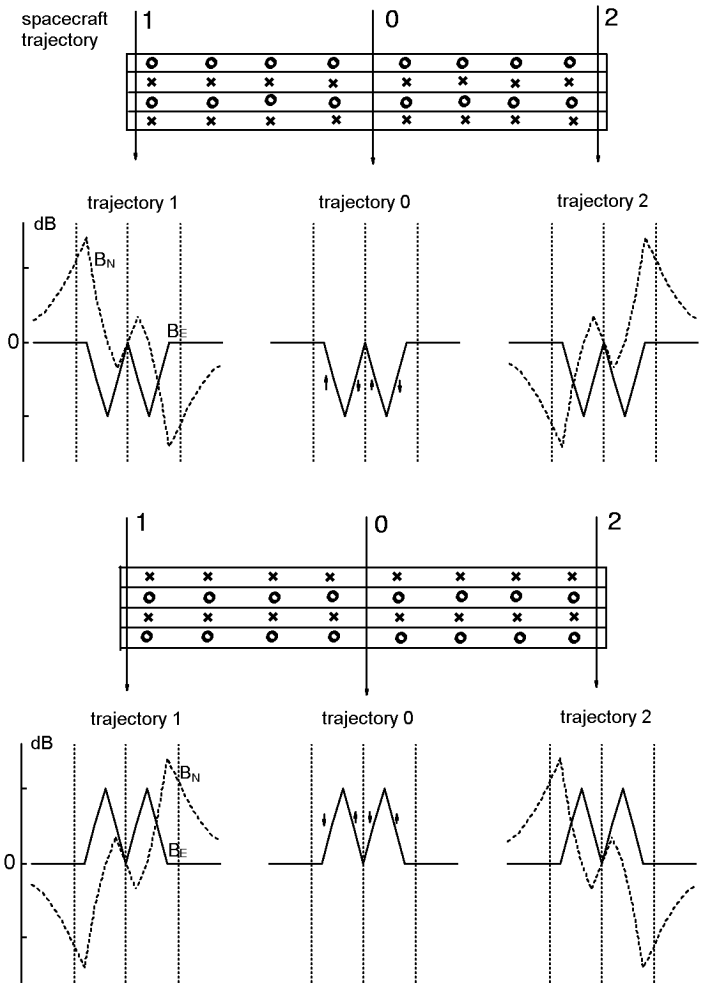

Figure 4. Same as Figure 1 (in the case of four sheets).

the current sheet. Variations of the east-west magnetic component are irrespective of whether the satellite crosses the current sheets far from the edges (track 0 in all figures) or close to them (for example, tracks 1 and 2).

In contrast, the north-south component B_N is strongly dependent on the edge positions. B_N is close to zero far from the sheet edges (track 0), and this peculiarity is solid evidence of the azimuthally extended current sheets. B_N shows the distinctive features of opposite sign at the morning and evening edges of the current sheets (tracks 1 and 2). One peaked wave is typical of one current sheet: it can be negative or positive, depending on the sort of edge and direction of currents. The sine wave is typical of two current sheets; the double-humped positive or negative wave is for three sheets; and two sine waves occurring against the background of an increasing or decreasing magnetic field are typical of four current sheets. Thus the meridional magnetic component B_N is evident on the sheet edges, in addition to the information on the number and polarities of current sheets.

Examples of two and three consecutive and parallel sheets with displaced edges are given in Figure 2, tracks 3–8. As before, the B_E component (solid line) shows the polarity of current sheets: the negative peaked wave is observed for upward/downward current sheets, and the positive peaked wave is for downward/upward current sheets. The B_N component (dotted line) takes the form of a smoothed wave in this case. It testifies the location of the current sheet edges (dawn or dusk), the maximum in the B_N component being displaced relative to the maximum in the B_E component. The opposite regularity is true for the inverse location of the sheet edges. The sign of the magnetic B_N component is determined by mutual disposition of the upward and downward field-aligned currents. Figure 3, tracks 3–8, shows the behavior of zonal B_E and meridional B_N components of magnetic perturbations in the case of three current sheets with displaced edges.

The specific case of the orthogonal track without the crossing of current sheets can be observed when the spacecraft moves along the meridian just in a gap between oppositely directed current sheets. One can see that in this case, only the B_N component shows a distinguishing characteristic, whereas component B_E is held close to zero (Figure 1, track 9). If the spacecraft crosses the current sheets far from the edges but at obtuse or acute angle, the B_E component

shows generally the same regularity as for the orthogonal crossing, although the differentials are flattened out. However, the B_N component in this case increases or decreases along the track, depending on the angle of inclination between the spacecraft orbit and the current sheets.

Therefore the east-west component provides reliable information on the number and polarity of the current sheets irrespective of the spacecraft orbit angle and the proximity of the sheet edges. The edge effects (or effects of increasing current density) can be identified solely from the north-south component B_N if the spacecraft crosses the current sheets not far from the edges. Thus examination of distinctive changes in both B_E and B_N magnetic components, observed along the spacecraft track, provides reliable signatures for the identification of current sheet structures: number and polarity of the current sheets, mutual disposition of the current edges, and spacecraft orbit inclination to current sheets. In doing so, it should be borne in mind that disturbances, observed by satellites, are produced mainly by currents flowing in the nearest vicinity of the satellite orbit.

3. Numerical Procedure for Reconstruction of the Real FAC Structure

General regularities in variations of B_E and B_N components of the magnetic field, typical of the different structures of current sheets, give us a background for the recognition of FAC patterns observed in the course of spacecraft passes through the dayside cusp region. The recognition is realized by the method of model calculation and successive approximation of calculated patterns of magnetic disturbances to the observed patterns. Magnetic data of the spacecraft magnetometers show large-scale and small-scale fluctuations. Preparatory smoothing or a filtration procedure is necessary. To distinguish the large-scale FAC effects, a simple linear filter is used. After filtration, smoothing curves with local maximums and minimums are derived (not shown in Figures 6–8.) The problem of the best fitting of the curves calculated for model patterns to the actual observed profiles for the meridional (or zonal) component of the magnetic field perturbation is solved by finding the smallest value for the function

$$f(x) = \sum_{i=1}^{N} [B_i^{(\exp)} - B_i(x)]^2 \qquad x = (j_1, \ldots, j_n) \quad (5)$$

where N is the number of one-dimensional grid points along the spacecraft trajectory projection and $\{x\}$ is a set of unknown parameters of n current sheets. $B_i^{(\exp)}$ is the magnitude of actual observed magnetic field disturbances (B_E or B_N components) at a point (i) and $B_i(x)$ is the computing component. The function $B_i(x)$ can be written as Taylor series

$$B_i(x) = B_i(x^{(0)}) + \frac{\partial B_i(x^{(0)})}{\partial x_1}\Delta x_1 + \ldots + \frac{\partial B_i(x^{(0)})}{\partial x_n}\Delta x_n \quad (6)$$

where $x^{(0)}$ is the zero-order approximation of parameters. The computing and actual profiles of a magnetic disturbance are fitted while minimizing the function

$$f(x) = \sum_{i=1}^{N} \Big[B_i^{(\exp)} - B_i(x^{(0)}) - \frac{\partial B_i(x^{(0)})}{\partial x_1}\Delta x_1 - \ldots - \frac{\partial B_i(x^{(0)})}{\partial x_n}\Delta x_n \Big]^2 \quad (7)$$

Minimization of function (7) is reduced to solution of the system of n linear algebraic equations for local minimums when $x_i = J_i$, $\Delta x_i = J_i - J_i^{(0)}$ and J_i is current density in the i sheet. As a result, a set of optimal current parameters providing the best fitting of the experimental and calculated profiles is determined. A practical inversion algorithm for the determination of current structures is based on numerical solution of the two-dimensional equation (3) and consists of three consecutive steps (or approximations), as follows: (1) The distribution of only the zonal component of magnetic disturbance B_E is analyzed. As a result of computer simulation, the current structure is adopted, which provides the best fitting of the observed and calculated trends of B_E along the satellite path. Parameters of hypothetical current sheets such as polarity and latitudinal width are stated on the assumption that these sheets are extended from dusk to dawn. The relative intensity of currents in each sheet is obtained from expression (7). (2) The only meridional component B_N is analyzed. The number of current sheets is specified from results of the previous step, each current sheet being cut in the vicinity of the spacecraft trajectory. The position of current sheet edges ensuring the best fitting of experimental and calculated profiles of B_N is chosen as actual. (3) The additional current sheets uncrossed by the spacecraft trajectory are included in the analysis to improve the fitting of B_N profiles. Parameters of additional sheets are selected to ensure the minimum discrepancy between experimental and calculated B_N profiles.

4. Application of the Algorithm to AUREOL 3 Magnetic Data

Four consecutive AUREOL 3 tracks on October 14, 1981, when the spacecraft crossed the northern daytime cusp region are examined. Figure 5 shows the IMF parameters in the period of these crossings. The B_y IMF was negative in the course of two first crossings and close to zero in the course of two last crossings, whereas the vertical component B_z was close to zero for the first track, southward for second track, and positive for the two last tracks. The spacecraft moved under a very small angle to the noon-midnight meridian. Figures 6, 7, 8, and 9 (left side) illustrate the satellite-measured (solid lines) and calculated (dotted lines) profiles of zonal B_E and meridional B_N components of magnetic perturbations for tracks 307N, 308N, 309N, and 310N, correspondingly. Indications of universal time (UT), height (h), magnetic local time (MLT), and invariant latitude (ILAT) are given for each track as well. The right-hand side of Figures 6–9 shows the corresponding FAC patterns, ensuring the best fitting of experimental and calculated profiles.

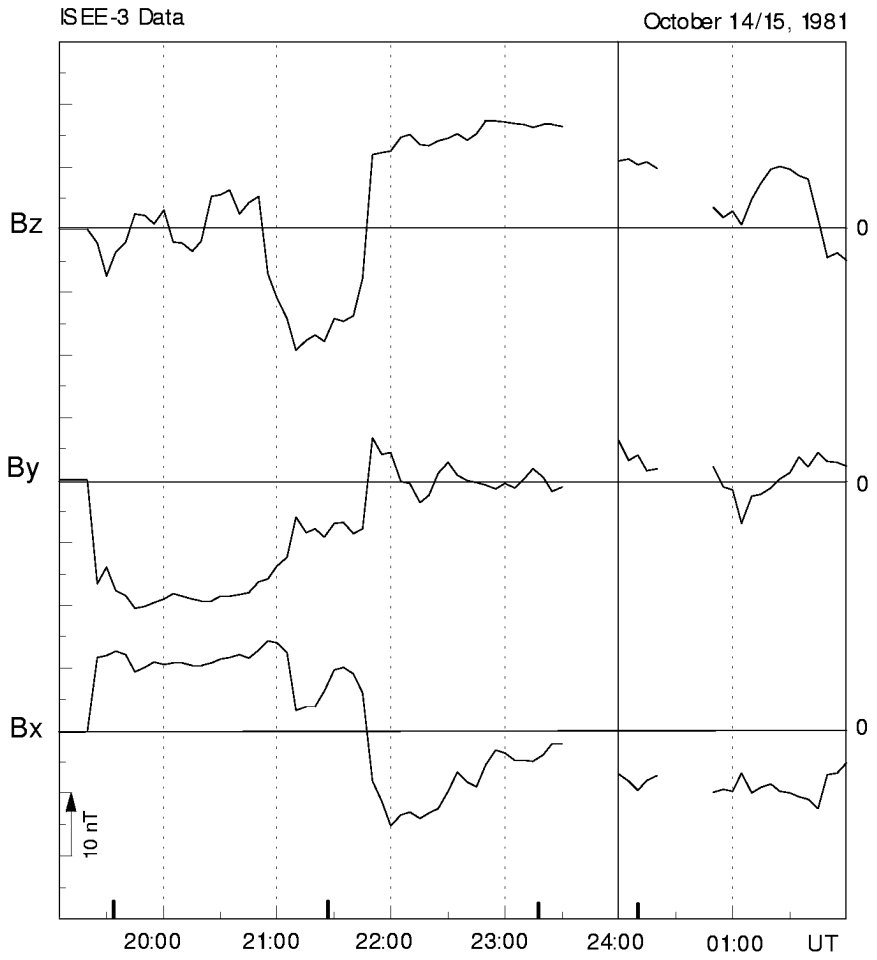

Figure 5. Interplanetary magnetic field, October 14–15, 1981, ISEE 3 data.

Figure part a, b, c are for the first, second, and third approximations in the framework of the described algorithm. Only large-scale structures of the field-aligned currents are examined in our analysis, although there is no question that spacecraft data are evidence for smaller-scale current layers as well (see, for example, orbits 307N and 308N). Some parameters of calculated large-scale current patterns (number of current sheets and relative intensity of currents) are given in Table 1. To derive density the 0.2 (mkA m^{-2}) coefficient might be applied. The estimation of discrepancy between the actually observed (without smoothing) curve $B_i^{(\exp)}$ and the calculated B_i has been carried out. The smallest value of

$$\sigma = \sum_{i=1}^{N} [(B_i^{(\exp)} - B_i)/B_i^{(\exp)}]^2$$

The profile of magnetic perturbation in the case of orbit 307N consists of one negative peaked wave in B_E and one negative peaked wave in B_N. These waves are rather flat and change almost synchronously. These peculiarities of the profile are described by three current sheets with displaced edges, the upflowing currents being located in the equatorward sheet in the afternoon sector, and the downflowing currents being located in the intermediate sheet in the prenoon sector and in the poleward sheet in the afternoon sector. As Figure 6 shows, the best fitting of the observed and calculated profiles of magnetic perturbations is attained if one more wide sheet with upflowing weak currents is assumed to be located outside of the spacecraft trajectory in the dawn sector. Magnetic signatures for orbit 308N (Figure 7) are typical of two up/down current sheets crossed near their westward edge: one negative peaked wave in B_E and the sine wave in B_N. In general, the FAC structures derived for tracks 307N and 308N are rather similar, their main feature in the afternoon sector is the upflowing currents located at 75°–80°(ILAT and the downflowing currents located at higher latitudes. The FAC structure of this kind is typical of patterns of the field-aligned currents in the northern cusp region under conditions of the southward and large negative IMF components [*Iijima and Potemra*, 1976; *McDiarmid et al.,* 1979; *Troshichev et al.,* 1982].

The FAC structure observed for tracks 309N and 310N is of greater interest, since in this case, we deal with conditions of the northward IMF. Unfortunately, data from track 309N are not provided for latitudes higher than 82° ILAT, whereas data from track 310N are not available at latitudes

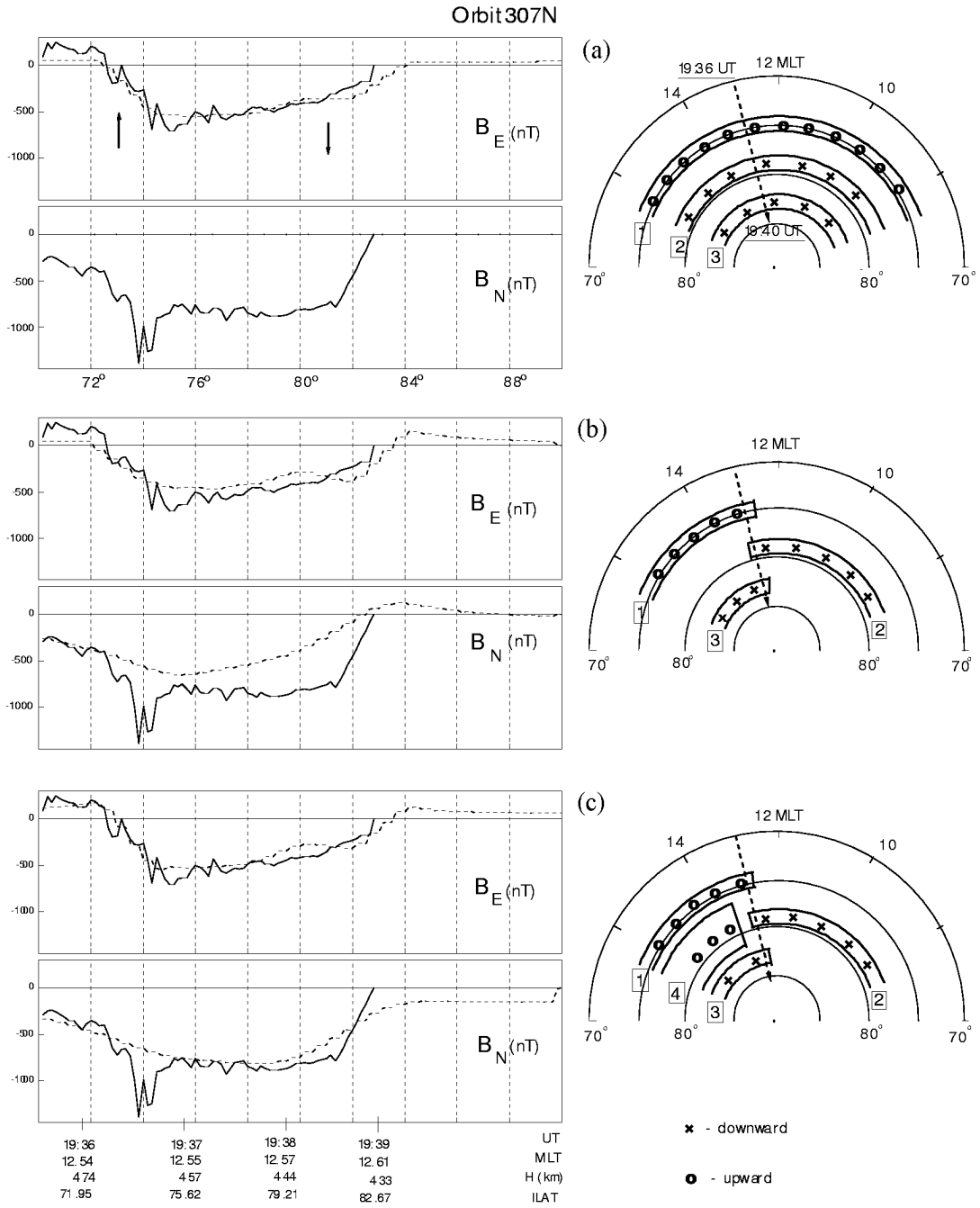

Figure 6. Actual observed (solid line) and calculated (dotted line) profiles of east-west B_{E}, north-south B_{N} components of magnetic field along track 307N, and appropriate FAC structures: (a) first, (b) second, (c) final approximation.

lower than 72° ILAT. However, we can regard data from these tracks as complementing each other, bearing in mind that they were obtained under similar IMF conditions. Track 309N (Figure 8) shows signatures of two main sheets in the afternoon sector, with the upflowing currents at the equatorward side (< 79° ILAT) and the downflowing currents at the poleward side (> 79° ILAT). In spite of it, two additional sheets in the prenoon sector, with the upflowing current at 80° ILAT and the downflowing current at higher latitudes, ensure the best agreement between the calculated and the experimental profiles of B_{N}, profile B_{E} being practically invariable. Track 310N indicates the downflowing currents at latitudes less than 80° ILAT and upflowing currents at latitudes 80°–84° ILAT, the current sheets being crossed

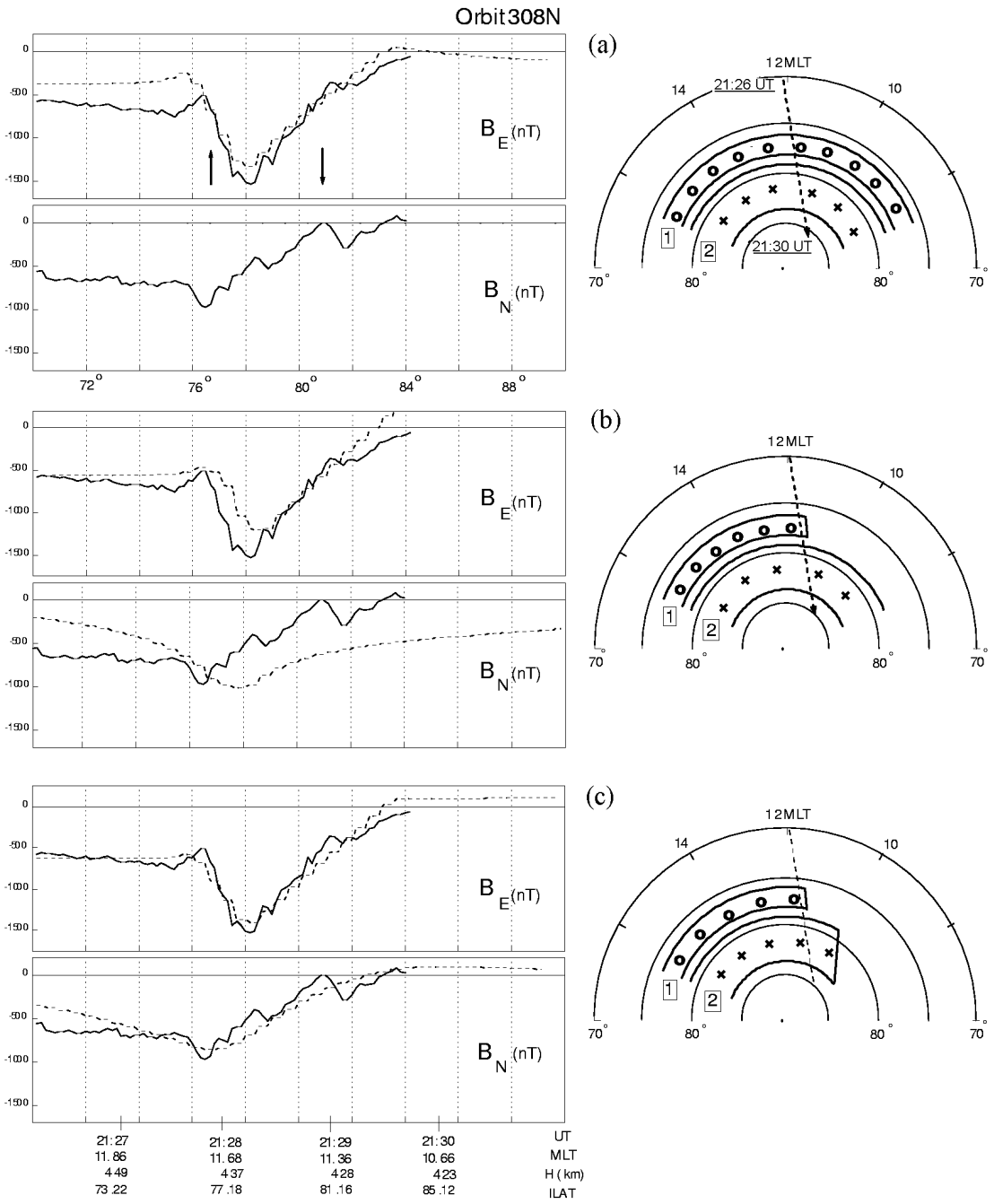

Figure 7. Same as Figure 6 but for track 308N.

near their westward edge. The best fitting of the observed and calculated profiles of magnetic perturbations for track 310N is attained if we assume availability of two additional sheets with oppositely directed currents in the prenoon sector (see Figure 9). Therefore we conclude that spacecraft AUREOL 3, crossing the northern daytime cusp region under conditions $B_z \geq 0$, $B_y \approx 0$ approximately along the noon meridian, met three current sheets. The most equatorward sheet, with the upflowing currents in the afternoon sector observed at orbit 309N, evidently falls into the category of Region 1 FAC. The farther intermediate sheet, located at latitudes about 80° (orbit 309N) or 76° − −79° (orbit 310N) with currents opposite in direction to those in Region 1, can be regarded as the proper cusp FAC system, and the most poleward sheet of currents observed at orbit 310N, upflowing in the afternoon sector and the downflowing in the prenoon and afternoon sectors, is evidently the mantle FAC system. The pairs of oppositely directed currents in the last two sheets are separated by a gap in the field-aligned currents located at the noon meridian.

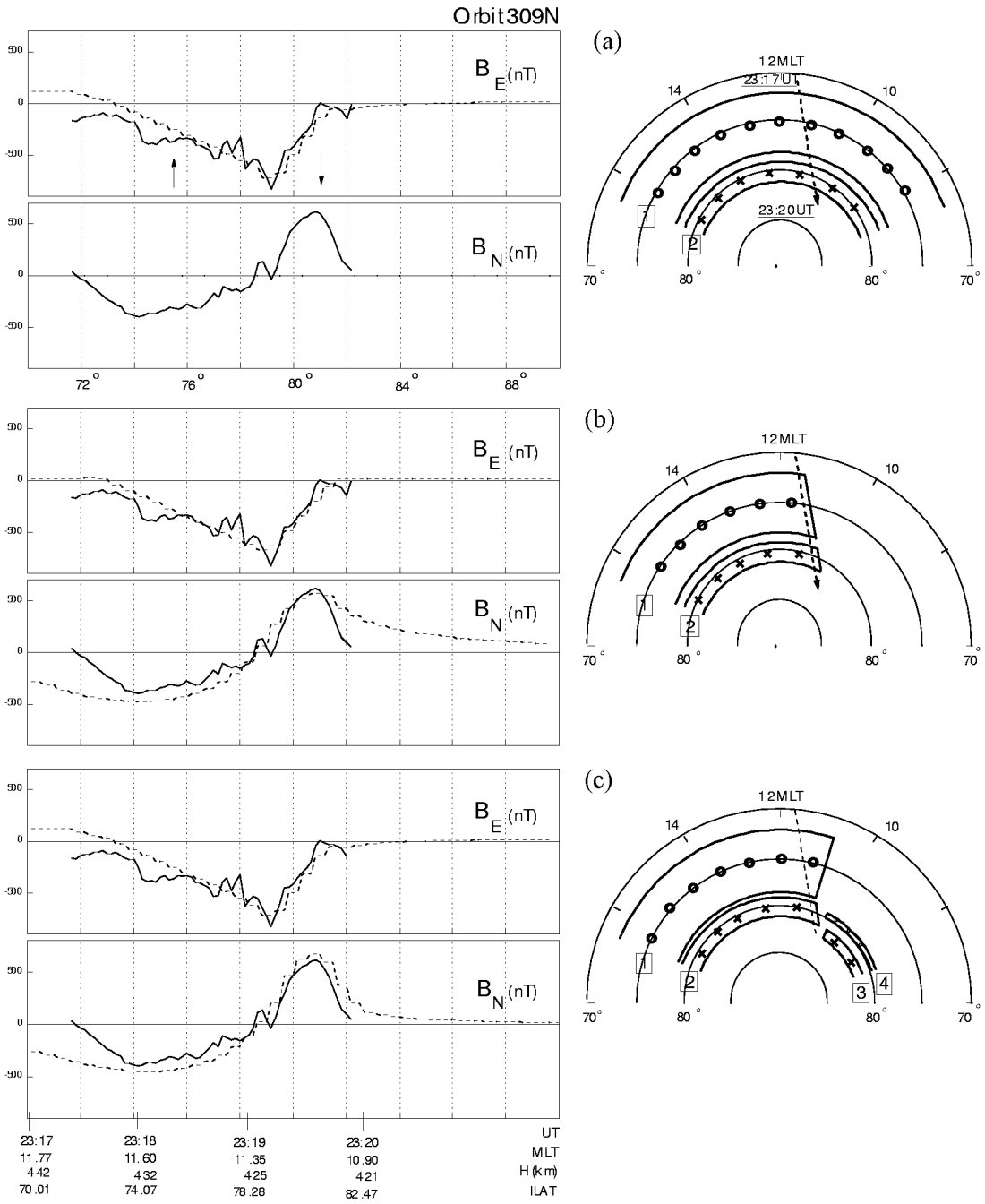

Figure 8. Same as Figure 6 but for track 309N.

5. Discussion

Patterns of the field-aligned currents, generated in the northern daytime cusp region under the influence of azimuthal B_y or northward B_z IMF components, were presented in recent years by *Erlandson et al.* [1988], *Saunders* [1992] and by *Yamauchi et al.* [1993], *Taguchi et al.* [1993], *Ohtani et al.* [1995a, 1995b], *Troshichev et al.* [1996]. The FAC pattern given by *Erlandson et al.* [1988] is evolution of concept presented in the studies of *Iijima and Potemra* [1976], *D'Angelo* [1980], and *Troshichev et al.* [1982] consists of the traditional Regions 1 and 2 field-aligned currents and cusp currents located poleward of Region 1 and named "mantle" current. Mantle current flows into the ionosphere in the afternoon sector and away from the ionosphere in the prenoon sector irrespective of the sign of B_y. The influence of the IMF azimuthal component shows itself mainly in the partial extent of Region 1 and mantle currents, shifted in pairs across local noon in association with B_y. A similar

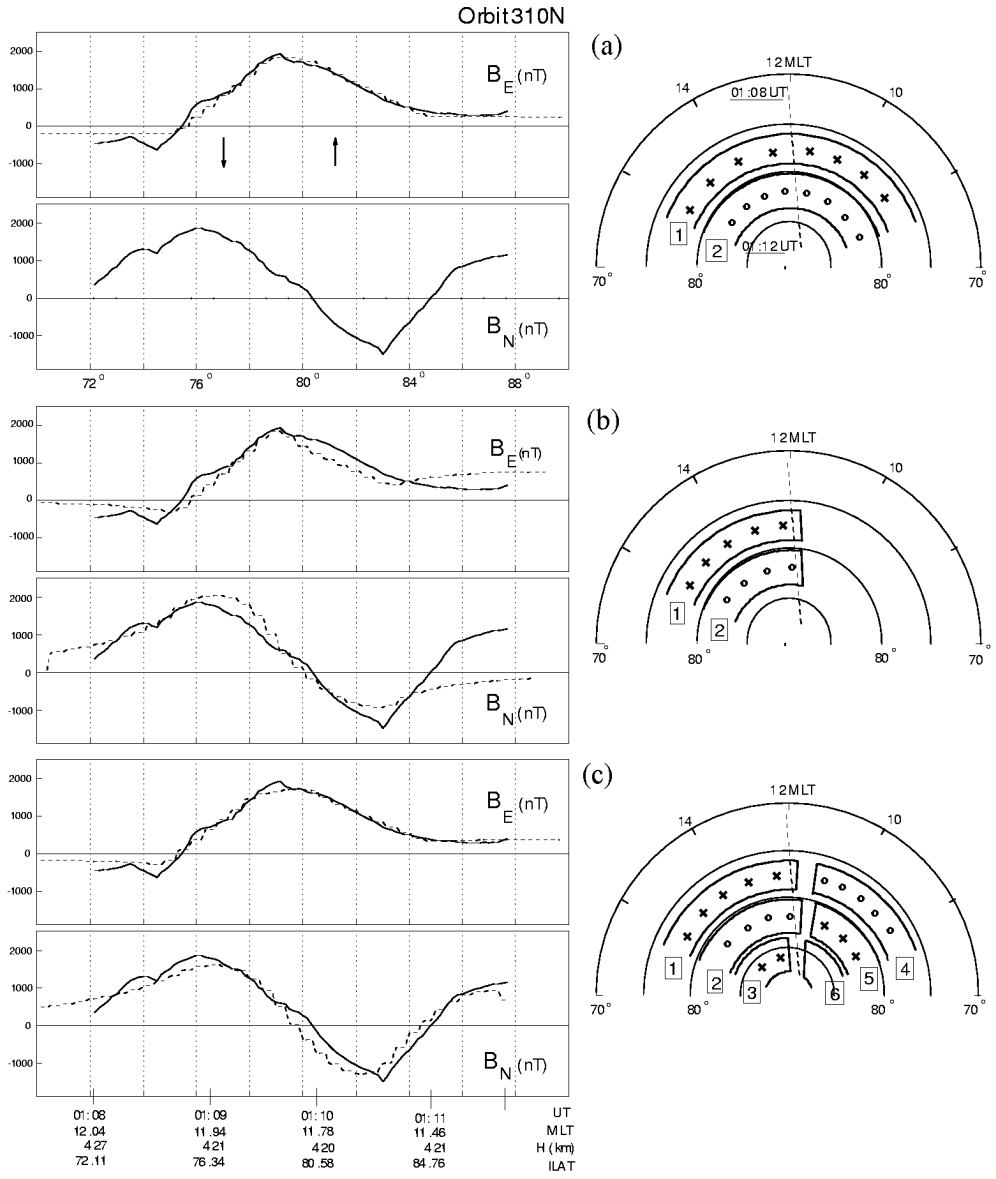

Figure 9. Same as Figure 6 but for track 310N.

current pattern is presented in the study of *Ohtani et al.* [1995a], where the term "Region 0" is used to refer to any FAC system poleward of Region 1 currents. The pattern of *Taguchi et al.* [1993] includes, along with Regions 1 and 2, the additional two layers of Birkeland currents in the noon sector with flow directions specified by B_y. This double current system is always located poleward of Region 1. As a result, the spacecraft intersecting the polar region in the prenoon or afternoon hours should meet four current sheets. Indeed, the four-current sheet structure was observed in the prenoon sector, when the IMF B_y component was negative [*Ohtani et al.,* 1995b]. The model of *Troshichev et al.* [1996], obtained on the basis of ground magnetic data, can be regarded as an intermediate between patterns proposed by *Erlandson et al.* [1988] and *Taguchi et al.* [1993]. This model assumes that the low-latitude cusp current sheet in the additional pair of Birkeland currents [see *Taguchi et al.,* 1993] is adjacent to Region 1 on the morning or on the evening side, depending on the sign of B_y.

The patterns of *Saunders* [1992], *Yamauchi et al.* [1993], and *de la Beaujardiere et al.* [1993] develop the concept proposed at first by *McDiarmid et al.* [1979]. These patterns consider the field-aligned currents observed in the cusp region as an extension of the Region 1 currents to the noon sector under the influence of IMF B_y.

Let us compare the patterns mentioned above with the FAC structures derived from observations of magnetic perturbations onboard the AUREOL 3 spacecraft under conditions of the northward IMF and B_y close to zero. Firstly, it is necessary to note that FAC systems, presented in Figures 8

Table 1. Parameters of the Current Pattern

	Orbit									
	307N	307N	307N	307N			308N	308N		
Sheet number	1	2	3	4			1	2		
Relative intensity	−6.5	1.9	5.2	−2			−3.5	7.3		
	Orbit									
	309N	309N	309N	309N	310N	310N	310N	310N	310N	310N
Sheet number	1	2	3	4	1	2	3	4	5	6
Relative density	−3.2	7.5	6	−7.8	−15	−12.5	4.5	−5.6	9	−3.3

and 9, suggest the FAC pattern with quasi-symmetrical distribution of pairs of oppositely directed currents relative to the noon meridian in each sheet. It implies that currents in all sheets in the cusp region change their direction when crossing the noon meridian, so that the gap in the field-aligned currents takes place at noon for $B_y = 0$. It would appear reasonable to infer that this gap displaces under the influence of the nonzero B_y toward dawn or dusk. This feature is extremely important for testing the FAC models in the daytime cusp region. It means that the concept of the cusp-current sheet as the westward or eastward extension of Region 1 currents [*McDiarmid et al.,* 1979] is inapplicable.

Secondly, the FAC systems, presented in Figures 8 and 9, suggest the FAC pattern with two sheets containing the pairs of oppositely directed currents poleward from the traditional Region 1 FAC. It means that a two-layer current structure is available instead of a single zone of "mantle" currents [*Erlandson et al.,* 1988] or "Region 0" [*Ohtani et al.,* 1995a]. Taking into account Region 2 FAC observed at latitudes lower than 75° in the dawn and dusk sectors but invisible at noon meridian, we can speak about the four-layer current structure. Note that a four-layer structure with the oppositely directed currents (Region 2, Region 1 and two additional layers poleward of Region 1) has been presented in the patterns of *Taguchi et al.* [1993] and *Ohtani et al.* [1995b]. However, this structure was regarded as typical of only one, dawn or dusk, MLT sector, depending on the sign of B_y. Our results, obtained for the conditions of $B_y = 0$, suggest that a two-layer current structure poleward of Region 1 can be observed in the prenoon and afternoon MLT sectors of the polar region simultaneously. The FAC pattern in the daytime cusp region summarizing our results for conditions $B_z > 0$, $B_y \approx 0$ is presented in Figure 10.

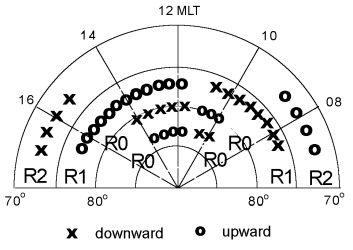

Figure 10. FAC pattern in the daytime cusp region for IMF $B_z > 0$ and $B_y \approx 0$.

The current patterns presented in this study were constructed on the basis of isolated spacecraft traverses through the cusp/cleft region as in the overwhelming majority of patterns in other studies mentioned here. Adoption of the statistically significant set of data is required to approve the obtained results. However, there is no question that use of the meridional component of magnetic perturbations in analyzes of the FAC current structure provides new and important information on the edge effects and gaps in the current sheets. This information is especially important for determination of the FAC pattern in the daytime cusp region.

6. Conclusion

The algorithm for interpretation of spacecraft observations of the large-scale field-aligned currents is proposed, the zonal and meridional components of the magnetic field perturbations being used in the analysis. While a zonal component specifies the number, polarity, and latitudinal width of FAC sheets, a meridional component is evidence of edges and gaps in the current sheets. The last circumstance is especially important for the daytime cusp region where Region 1 FACs are terminated in the vicinity of the noon meridian, whereas current sheets located poleward of Region 1 (i.e., cusp currents) are evidently confined to the limited MLT sector. The algorithm ensures automated derivation of the "two-dimensional" FAC structure in the region of spacecraft trajectory in assuming that the current sheets are located along the latitude. Four consecutive AUREOL 3 spacecraft intersections of the northern daytime cusp region have been used as an experimental basis for the analysis. It is concluded that the specific FAC system located poleward of Region 1 is typical of conditions $B_z > 0$ and $B_y = 0$. The system consists of two current sheets with pairs of oppositely directed currents separated by gaps at the noon meridian, and therefore cannot be regarded as an extension of Region 1 currents from other local times.

References

D'Angelo, N., Field-aligned currents and large scale magnetospheric electric fields, *Ann. Geophys., 36*, 31, 1980.

de la Beaujardiere, O., J. Watermann, P. T. Newell, and F. J. Rich, Relationship between Birkeland current regions, particle precipitation, and electric fields, *J. Geophys. Res., 98*, 7711, 1993.

Doyle, M. A., F. J. Rich, W. J. Burke, and M. Smiddy, Field-aligned currents and electric field observed in the region of the dayside cusp, *J. Geophys. Res., 86*, 5656, 1981.

Erlandson, R. E., L. J. Zanetti, T. A. Potemra, P. F. Bythrow, and R. Lundin, IMF B_y dependence of Region 1 Birkeland currents near noon, *J. Geophys. Res., 93,* 9804, 1988.

Friis-Christensen, E., Y. Kamide, A. D. Richmond, and S. Matsushita, Interplanetary magnetic field control of high-latitude electric fields and currents determined from Greenland magnetometer data, *J. Geophys. Res., 90*, 1325, 1985.

Iijima, T., and T. A. Potemra, Field-aligned currents in the dayside cusp observed by TRIAD, *J. Geophys. Res., 81*, 5971, 1976.

Levitin, A. E., R. G. Afonina, B. A. Belov, and Y. I. Feldstein, Geomagnetic variation and field-aligned currents at the northern high-latitudes and their relations to the solar wind parameters, *Philos. Trans. R. Soc. London, Ser. A, 304*, 253, 1982.

Lukianova, R. Y., Convection systems in the dayside polar cap produced by various patterns of the cusp field-aligned currents, *Phys. Chem. Earth, 22*, 7–8, 751, 1997.

McDiarmid, I. B., J. R. Burrows, and M. D. Wilson, Large-scale magnetic field perturbations and particle measurements at 1400 km on the dayside, *J. Geophys Res., 84*, 1431, 1979.

Ohtani, S., T. A. Potemra, P. T. Newell, L. J. Zanetti, T. Iijima, M. Watanabe, M. Yamauchi, R. D. Elphinstone, O. de la Beaujardiere, and L. G. Blomberg, Simultaneous prenoon and postnoon observations of three field-aligned current systems from Viking and DMSP-F7, *J. Geophys. Res., 100*, 119, 1995a.

Ohtani, S., et al., Four large-scale field-aligned current systems in the dayside high-latitude region, *J. Geophys. Res., 100*, 137, 1995b.

Saflekos, N. A., R. E. Sheehan, and R. L. Carovillano, Global nature of field-aligned currents and their relation to auroral phenomena, *Rev. Geophys. and Space Phys., 20*, 709, 1982.

Saunders, M. A., The morphology of dayside Birkeland currents, *J. Atmos. Sol. Terr. Phys., 54*, 457, 1992.

Taguchi, S., M. Sugiura, J. D. Winningham, and J. A. Slavin, Characterization of the IMF B_y-dependent field-aligned currents in the cleft region based on DE 2 observation, *J. Geophys. Res., 98*, 1393, 1993.

Troshichev, O. A., V. A. Gizler, and A. V. Shirochkov, Field-aligned currents and magnetic disturbance in the dayside polar region, *Planet. Space Sci., 30*, 1033, 1982.

Troshichev, O. A., A. L. Kotikov, E. M. Shishkina, B. D. Bolotinskaya, E. Friis-Christensen, and S. Vennerstorm, Substorm activity precursors in the dayside magnetic perturbations, *J. Atmos. Sol. Terr. Phys., 58*, 1293, 1996.

Watanabe, M., T. Iijima, and F. J. Rich, Synthesis model of dayside field-aligned currents for strong interplanetary magnetic field B_y, *J. Geophys. Res., 101*, 13,303, 1996.

Yamauchi, M., R. Lundin, and J. Woch, The interplanetary magnetic field B_y effects on large-scale field-aligned currents near local noon: Contribution from cusp part and noncusp part, *J. Geophys. Res., 98*, 5761, 1993.

R. Lukianova and O. Troshichev, Arctic and Antarctic Research Institute, St. Petersburg, Russia.

Yu. Galperin and N. Jorjio, Institute of Space Research, 84/32 Profsoyuznaya Str., Moscow 117810, Russia.

(Received July 15, 2000; revised July 31, 2001;
accepted October 21, 2001)